A New LEFM Based Description of Concrete Fracture and Size Effects

Kim Wallin

VTT Materials and Built Environment, P.O. Box 1000, FI-02044 VTT, Espoo, Finland
Kim.Wallin@vtt.fi

Abstract Concrete is a so called quasi-brittle material which, despite predominantly elastic material response, exhibits in tension loading a stable non-linear fracture response, when tested under displacement control. The reason for the non-linearity is the development of a fracture process zone, in front of the crack, due to micro-cracking and crack bridging. It has become increasingly popular to model the fracture process zone with different cohesive zone models. However, their use requires sophisticated finite element modeling and their success is directly related to the correctness of the assumed stress relaxation in the fracture process zone. An alternative is to use LEFM combined with an effective crack length. The effect of the fracture process zone is to make the specimen sense the crack as being longer than $a_0+\Delta a$. The fracture process zone causes thus an effective increase in the crack driving force but also the apparent fracture resistance increases since the fracture process zone effectively "blunts" the crack tip. This simple method, that does not require any finite element modeling, can be used as an aid to select the proper cohesive zone model for more sophisticated modeling.

Keywords Concrete fracture, size effect, fracture toughness, quasi-brittle materials, K-R.

1. Introduction

Concrete is a so called quasi-brittle material which, despite predominantly elastic material response, exhibits in tension loading a stable non-linear fracture response, when tested under displacement control (Fig. 1 [1]). The reason for the non-linearity is the development of a fracture process zone, in front of the crack, due to micro-cracking and crack bridging. An excellent review of the physical fracture process of concrete has been given in e.g. [2] and need not be covered here in any more detail. Here, the focus is on the fracture mechanical description of the effect of the fracture process zone on the structural behavior of the test specimen and prediction of size effects.

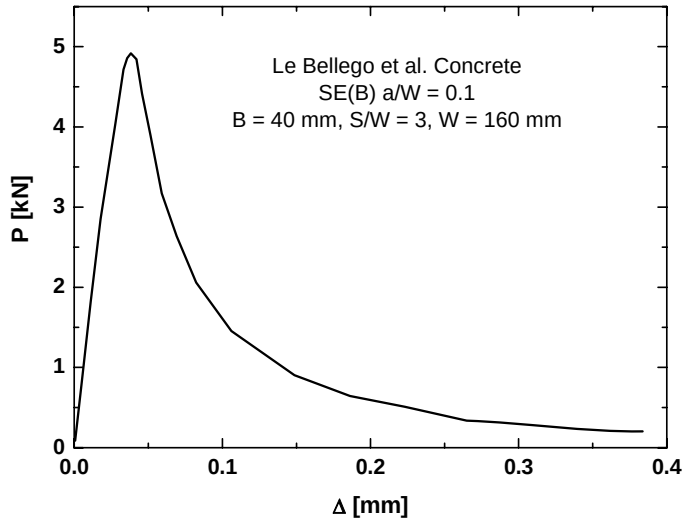

Figure 1. Example of a typical load-displacement relationship for concrete in a SE(B) fracture toughness test [1].

The cracking of concrete is schematically presented in Fig. 2. The shaded area in Fig. 2, relates to the micro-cracked material. The part of the micro-cracked material, lying in front of the macroscopic crack (including initial crack length a_0 and extended crack Δa), constitutes the active fracture process zone. In this region the material cohesion is weakened due to the micro-cracking. The effect of the fracture process zone is to make the specimen sense the crack as being longer than $a_0+\Delta a$. The fracture process zone causes thus an effective increase in the crack driving force. The effect of the fracture process zone is similar in nature to the Irwin plasticity correction [3] for metals.

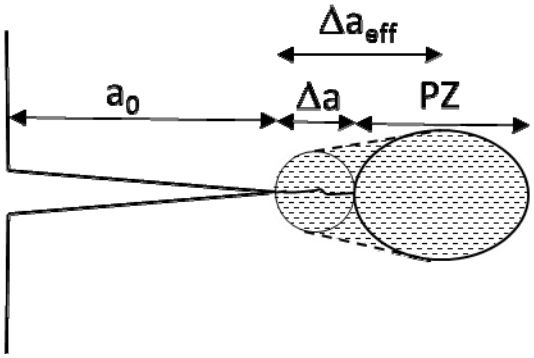

Figure 2. Schematic presentation of the fracture process of concrete. The initial crack length is a_0 and the macroscopic extended crack is Δa. PZ is the size of the active fracture process zone.

The part of the micro-cracked material that becomes engulfed in the crack wake, is no longer actively affecting the crack driving force, but it has absorbed energy related to the micro-crack surfaces. This has the effect of increasing the materials effective fracture resistance (Fig. 3).

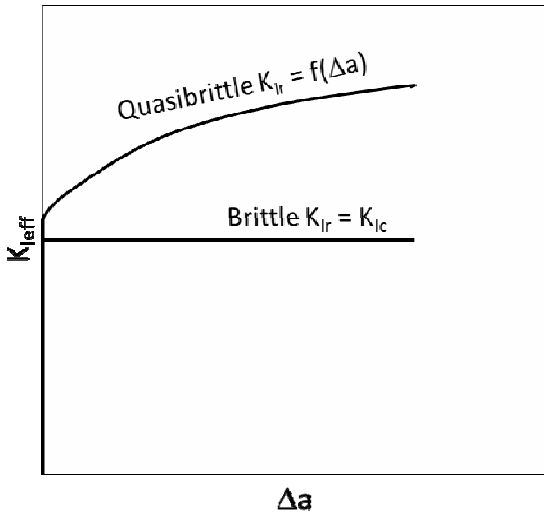

Figure 3. Schematic definition of the difference between an ideally brittle and a quasi-brittle material.

Often, fracture toughness tests of concrete are actually assessed by estimating an effective stress intensity factor and effective crack length [4], to derive an effective K-R curve in line with the ASTM E561 – 10 test standard [5]. This procedure is, however, not widely used, partly due to the question regarding the significance of the effective crack length and effective crack driving force. Another method called the double-K or double-G criterion is based on the estimate of the stress intensity at the onset of first crack extension (with a non-developed fracture process zone) and the

stress intensity corresponding to maximum load in the test [4]. This method is really an improvement of the classical tests where the maximum load has been combined with the initial crack length (a_0) to obtain a nominal fracture toughness value. The challenge with the double-K criterion lies in the reliable detection of the moment of crack initiation, which is almost invisible on the load-displacement record. Also, the estimation of the crack length at maximum load contains an experimental challenge and the necessity to combine both estimates of the crack tip displacement and load displacement. This prevents the method from becoming a simple quality assurance type of fracture toughness estimate.

As a compromise to the use of the classical nominal load maximum stress intensity factor, a special size effect expression has been proposed by Bažant. (See e.g. [6]). The Bažant size effect expression is versatile and has been shown to describe well the size effect in load maximum values of concrete and other quasi-brittle materials. The Bažant size effect expression for load maximum (P_{max}) can be expressed in the form of Eq. (1). B and W denote the fracture toughness specimen thickness and width and σ_f corresponds to the tensile stress of the material. The constant c accounts for specimen geometry and W_0 is a normalizing constant. The constants c and W_0 are determined by fitting to test results from different size specimens of identical geometry. Apparently the only weakness with the size effect expression is that a comparison between different loading geometries is not possible without the inclusion of additional fitting parameters [7].

$$\frac{P_{\max}}{B \cdot W} = \frac{c \cdot \sigma_f}{\sqrt{1 + \frac{W}{W_0}}}, \tag{1}$$

Here, a LEFM based estimate of the effective stress intensity factor and the effective crack growth at maximum load in a fracture mechanics test is used to obtain a simple power law approximation of the effective K-R curve that is applicable to the description of not only different size specimens, but also specimens with varying geometry.

2. Estimate of Maximum Load

In the case of metals, the materials tearing resistance is usually well described with a simple power law expression. Assuming, that the evolution of the fracture process zone and its effect on the effective materials fracture resistance behaves similarly to metals, also the effective stress intensity factor as a function of the effective crack growth should be possible to approximate with a power law in the form of Eq. (2).

$$K_{Ieff} \approx K_{1mm} \cdot \Delta a_{eff}^{m}, \tag{2}$$

For metals, when the tearing resistance is expressed in J-integral units, the power m is close to 0.5 or less. Thus, in K units the power should be in the vicinity of 0.25. If the fracture process zone size is very small compared to the crack growth, Δa, the power m will be small. If it is large compared to Δa, the power m should be closer to 0.25 or even above. When the relation between crack growth and fracture process zone no longer exists, the power m is expected to grow uncontrollable. This is not, however, expected to occur until well beyond the maximum load value.

The effective stress intensity factor is related to load and the effective crack length by Eq. (3).

$$K_{Ieff} = \frac{P}{B \cdot \sqrt{W}} \cdot f\left(\frac{a_0 + \Delta a_{eff}}{W}\right), \tag{3}$$

Eq. (3) differs from the classically used nominal stress intensity factor, which is calculated using only the initial crack size (a_0). The nominal stress intensity factor under-predicts the true effective crack driving force and should not be used in the assessment of quasi-brittle materials.

Combining Eqs. (2) and (3) leads to a relation between load and effective crack growth, Eq. (4).

$$P = \frac{K_{1mm} \cdot \Delta a_{eff}^{m} \cdot B \cdot \sqrt{W}}{f\left(\frac{a_0 + \Delta a_{eff}}{W}\right)}, \tag{4}$$

When the derivative of Eq. (4) (dP/da) is 0, the load and effective crack length correspond to maximum load. This leads to the relation between power m and effective crack extension in the form of Eq. (5) [8].

$$m = \frac{\Delta a_{effP\max}}{W} \cdot \frac{f'\left(\frac{a_0 + \Delta a_{effP\max}}{W}\right)}{f\left(\frac{a_0 + \Delta a_{effP\max}}{W}\right)}, \tag{5}$$

Eq. (5) is general and can be applied to any geometry for which the shape function f(a/W) is known. A numerical inversion of Eq. (5) is quite simple. One can tabulate a set of a_0, m and $\Delta a_{effPmax}$ values for a desired geometry and then a specific equation may be fitted to the data, or the information can be interpolated from the table. As an example, the solutions for the standard SE(B) and C(T) specimens are shown graphically in Figs 4a and b. An approximate solution for the standard SE(B) specimen with span width S/W = 4 is given by Eq. (6) and for the standard C(T) specimen with H/W = 0.6 is given in Eq. (7).

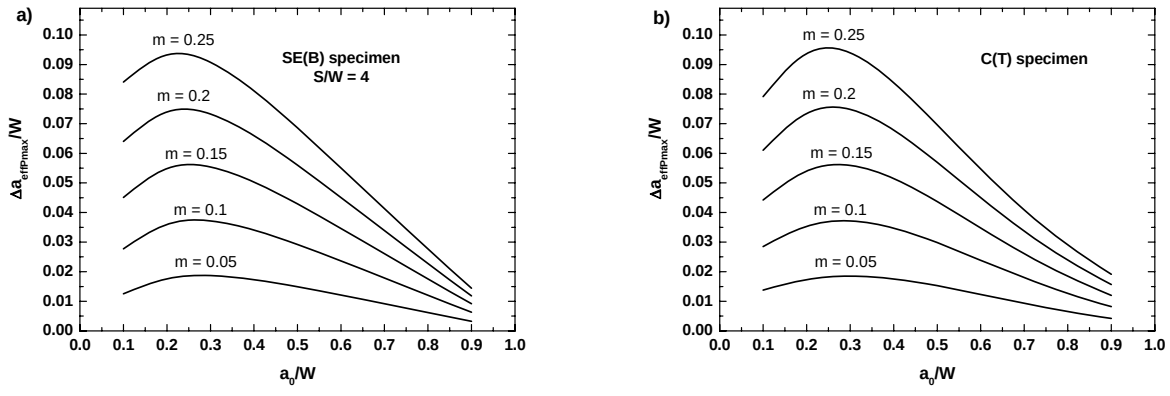

Figure 4. Effective crack growth corresponding to maximum load for standard SE(B) and C(T) specimens

$$\frac{\Delta a_{effP\max}}{W} \approx \frac{0.001118 + \left(\frac{a_0}{W}\right)^2 \cdot m - \left(\frac{a_0}{W}\right) \cdot m}{0.3886 \cdot \mathrm{m} - 0.1963 - \left(\frac{a_0}{W}\right) - 2.147 \cdot \left(\frac{a_0}{W}\right) \cdot \mathrm{m}} \qquad \left[\frac{S}{W} = 4, \frac{a_0}{W} \geq 0.1\right], \tag{6}$$

$$\frac{\Delta a_{effP\max}}{W} \approx \frac{m \cdot \sqrt{\frac{a_0}{W}}}{0.1542 + 8.063 \cdot \left(\frac{a_0}{W}\right)^2 \cdot m + exp\left\{2.94 \cdot \left(\frac{a_0}{W}\right)^2\right\} - 0.8219 \cdot m} \qquad \left[\frac{H}{W} = 0.6, \frac{a_0}{W} \geq 0.1\right], \tag{7}$$

It is important to note that Eqs. (6) and (7) are applicable only for standard specimen geometries. Especially in the case of the SE(B) specimen often different S/W ratios are used in the tests. For such tests, the standard f(a/W) expression can be adjusted e.g. by Eq. (8) [9] to be used together with its derivative in Eq. (5).

$$\mathrm{f}\left(\frac{\mathrm{a}}{\mathrm{W}}\right)_{\mathrm{S/W}} = \mathrm{f}\left(\frac{\mathrm{a}}{\mathrm{W}}\right)_{\mathrm{S/W=4}} \cdot \left\{1 + \left(1 - \frac{4\mathrm{W}}{\mathrm{S}}\right)\left(0.08\left(1 - \frac{\mathrm{a}}{\mathrm{W}}\right) + 0.24\left(1 - \frac{\mathrm{a}}{\mathrm{W}}\right)^2 - 0.28\left(1 - \frac{\mathrm{a}}{\mathrm{W}}\right)^3\right)\right\}, \tag{8}$$

The analysis consists of solving the power m and K_{1mm} iteratively by combining Eqs (4) and (5) to provide the correct maximum load values for different size and/or geometry specimens. The result is obtained in the form of the effective K-R curve in the form of Eq. (2) which then can be used for the evaluation of other geometries. For a constant geometry and fixed initial crack size ratio (a_0/W), the effective crack growth is directly related to the specimen width (W).

The proposed method relies on the assumption that the effective K-R curve up to maximum load can be approximated by a simple power law. Karihaloo and Nallathambi [10] collected a large number of SE(B) data and estimated from the experimental load-displacement traces, the relation between initial crack length and the effective (based on effective compliance) crack length corresponding to maximum load. Their results have been reproduced in Fig. 5.

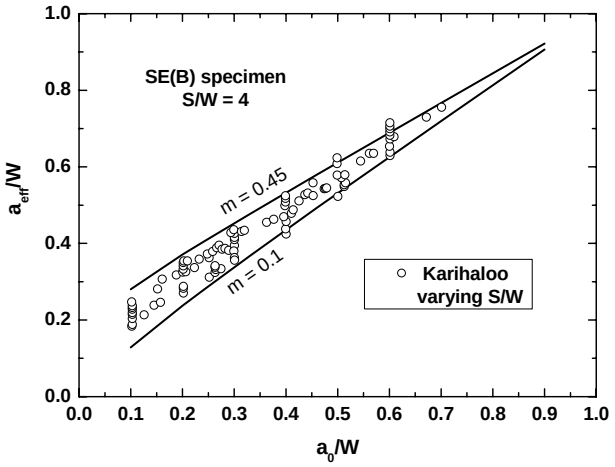

Figure 5. Estimate of effective crack length at maximum load, Eq. (6), compared to Karihaloo and Nallathambi experimental data from SE(B) specimens with varying S/W [10].

Included in the figure are theoretical estimates from Eq. (6) for the m values 0.1 and 0.45. It should be pointed out that the theoretical estimates are for a fixed span width of S/W = 4, whereas the Karihaloo and Nallathambi data contains specimens with varying span widths. A shorter span width increases the shear stresses in the specimen, having the effect of increasing the size of the fracture process zone. This translates into a larger m value. Overall, the Karihaloo and Nallathambi data provides a strong validation of Eq. (6) and the assumption that the effective K-R curve up to maximum load can be approximated by a simple power law.

3. Discussion

Fig. 6 compares the maximum load for varying crack length data from three different specimen sizes [11] are shown to be well described with a single effective K-R curve. Originally the smallest specimen size data was discarded as representing incomparable data due to a too small specimen size. Therefore the power law effective K-R curve was only fitted to the two larger specimen sizes. However, the use of the effective K-R curve describes well all three specimen sizes. Fig. 6 includes also another "small" specimen data set [12] representing the same type of concrete. The points denoted as squares with crosses lie very close to the other "small" specimen data (open squares), indicating that the fracture toughness of the concretes is similar.

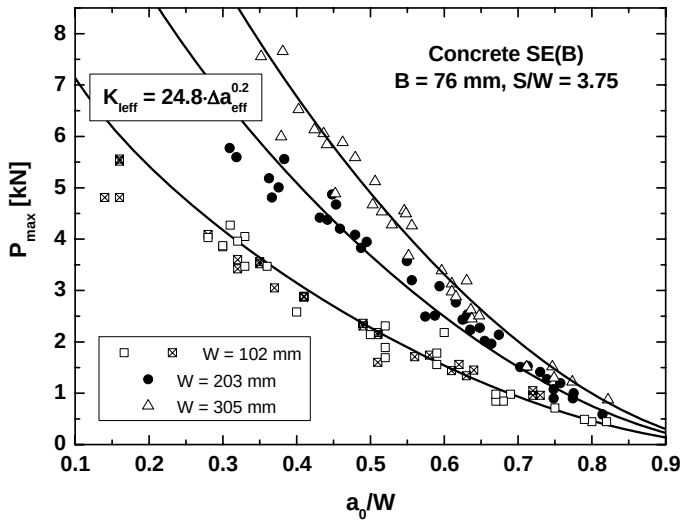

Figure 6. The maximum load for three different specimen sizes with strongly varying initial crack lengths are all described by a single K-R curve. The data has been taken from [11]. The squares marked by a cross are from [12], but their behavior is practically identical to the other specimens.

These examples show the descriptive power of the power law effective K-R curve estimated based on the maximum load values.

The effective K-R curve describes well the specimen behavior up to maximum load. This is exemplified in Fig. 7, where SE(B) data for limestone is analyzed. Fig. 7a, shows the maximum load values for self-similar specimens of different size [13]. Even though limestone differs from concrete, the fracture process is sufficiently similar to enable the use of limestone as an example. The power law K-R curve was fitted to the maximum load data in Fig. 7a. Then, the K-R curve estimate was used to predict the load displacement up to maximum load for the three different specimen sizes (Figs 7b, c, d). For the prediction, the crack is first advanced several small steps of Δa_{eff}. Next the K-R curve is used to estimate the K_{Ieff} and P corresponding to a + Δa_{eff}. Finally the

estimated load is used to calculate the displacement corresponding to a + Δa_{eff}, from the theoretical compliance. Considering the scatter of individual load-displacement traces, the prediction up to maximum load is excellent. Thus, this very simple power law K-R procedure can be used to predict the non-linearity in concrete and stone structures up to maximum load.

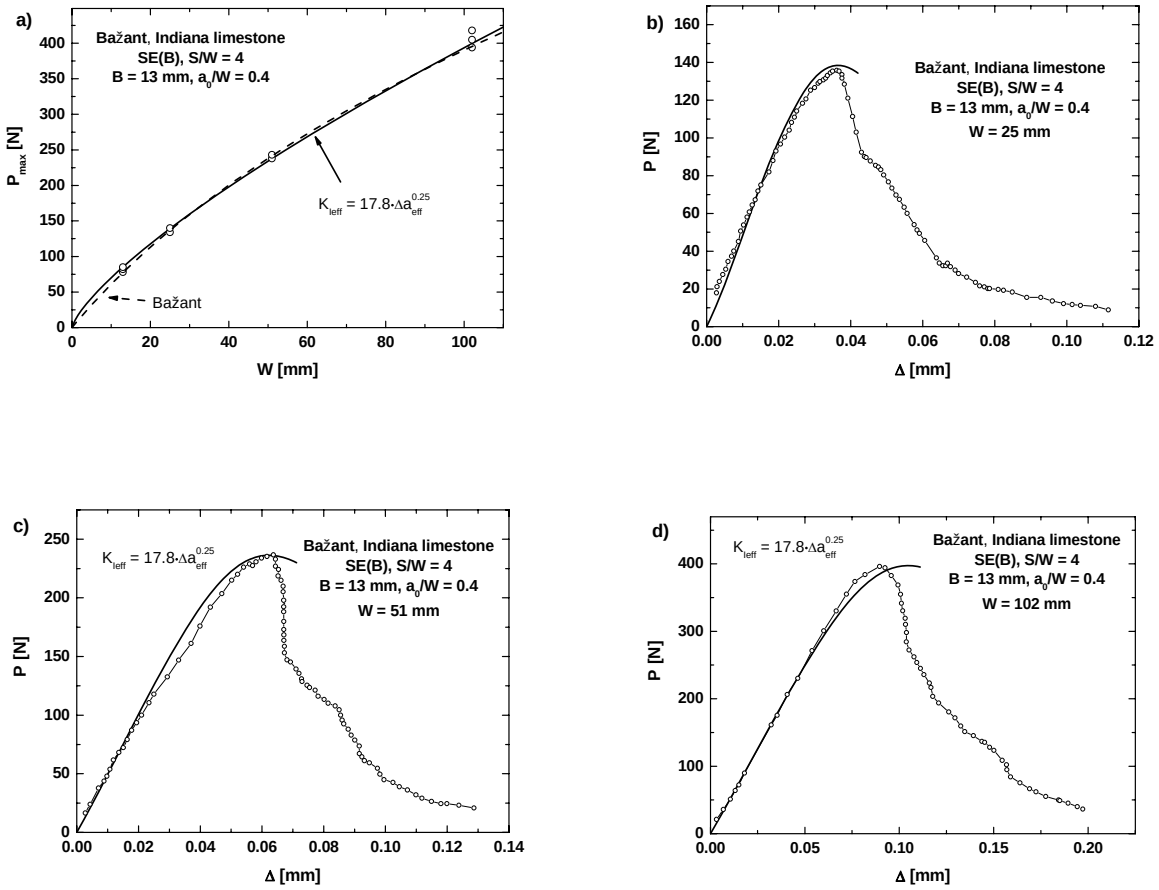

Figure 7. The prediction of load displacment dependence up to maximum load, based on simple effective K-R curve fitting to maximum load data. Data taken from [13].

Beyond maximum load, the connection between the effective crack length and the fracture process zone size breaks up. This is highlighted in Fig. 8. The load-displacement data was extracted from [1], so that for each specimen size representative upper and lower bound load-displacement traces were digitized. The effective crack length was estimated directly from the individual load-displacement data pairs, assuming that all the non-linearity is due to effective crack growth. Fig. 8a shows the effective crack driving force versus absolute effective crack growth and Fig. 8b shows the effective crack driving force versus proportional crack growth. Also included in the plots is the effective K-R curve estimated for the maximum load values. It is seen that for crack growth up to maximum load and slightly beyond, the effective K-R curve follows the absolute effective crack growth, whereas for large crack growths the effective K-R curve follows the proportional effective crack growth. This is a direct result of the fracture process zone evolution. Prior to maximum load, the fracture process zone is controlled by the fracture mechanical loading introduced by the crack. At some point, the connection between process zone size and the effective crack length breaks up. Finally, when the facture process zone has fully engulfed the crack and possibly extended to the free surface, the fracture process zone size develops as if there was no single crack in the structure.

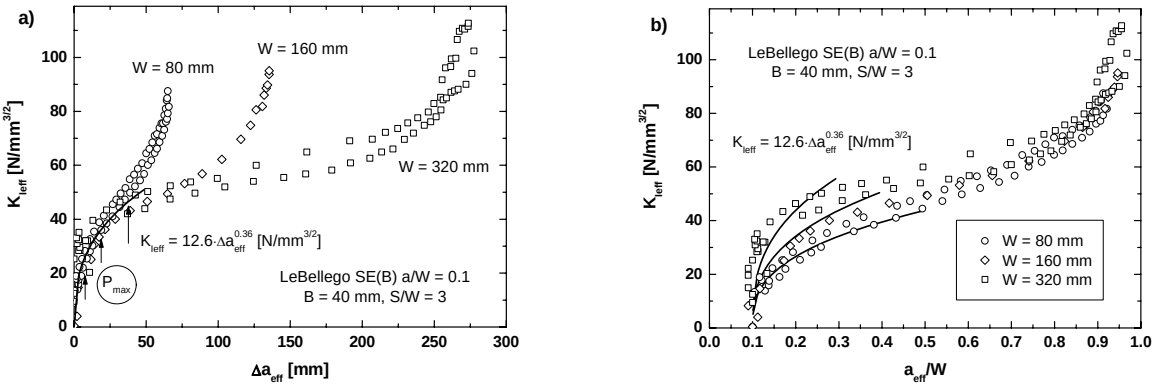

Figure 8. Normalization of effective crack driving force versus effective crack growth for self-similar SE(B) specimens of different size. Data extracted from [1]. Fig. 8a shows the effective crack driving force versus absolute effective crack growth and Fig. 8b shows the effective crack driving force versus proportional crack growth. Also included in the plots is the effective K-R curve estimated for the maximum load values.

The power law method contains similarities to an analytical cohesive zone method, which has been applied to describe the size effect in SE(B) specimens [14, 15]. The power law method is, however, much easier to use and provides an at least as good description of the size effect as can be seen by comparing Fig. (6) with Figs (4-6) in [15]. The advantage of the power law procedure lies in the very simple quantification of the fracture process zone development. A small power m indicates a brittle material, where the fracture process zone remains small throughout the fracture process. This is the case for m values of the order of 0.1 and below. The other extreme is a large m value in which case the material is crack insensitive and the damage comes mainly from the fracture process zone evolution. The method enables also the quantification of constraint in terms of the power m.

The procedure results in the estimate of the effective stress intensity factor corresponding to 1 mm effective crack growth.

4. Summary and Conclusions

Concrete is a so called quasi-brittle material which, despite predominantly elastic material response, exhibits in tension loading a stable non-linear fracture response, when tested under displacement control. The reason for the non-linearity is the development of a fracture process zone, in front of the crack, due to micro-cracking and crack bridging. The effect of the fracture process zone is to make the specimen sense the crack as being longer than $a_0+\Delta a$. The fracture process zone causes thus an effective increase in the crack driving force and apparent fracture resistance. The fracture modeling of concrete has been considered a mature theory. However, Present state of the art testing and assessment methods are somewhat cumbersome to use. Here, a LEFM based estimate of the effective stress intensity factor and the effective crack growth at maximum load in a fracture mechanics test is used to obtain a simple power law approximation of the effective K-R curve. It is shown that it is applicable to the description of not only different size specimens, but also specimens with varying geometry. The method is based on a new theoretical estimate of the effective crack growth corresponding to maximum load.

It can be concluded that:

- The presented procedure results in a simple two parameter description of the effective fracture resistance of quasibrittle materials.
- The procedure describes the effect of initial crack length on the maximum load values.
- The procedure enables the construction of the load-displacement dependence up to maximum load.
- The procedure enables a simple classification of the materials fracture process zone evolution.
- The procedure can be used in the context of the so called double-K criterion to describe the effective initiation toughness value.
- The procedure can be used to examine constraint effects on the materials fracture process zone evolution.
- In the future, the procedure may be used to assist damage mechanics type modeling of the failure of quasi-brittle materials.

Acknowledgements

This work has been part of the FAR project belonging to the SAFIR 2014 research program funded by VTT and by the State Nuclear Waste Management Fund (VYR), as well as other key organizations. The present work is connected to the quantification of constraint effects in brittle and quasi-brittle materials.

References

[1] C. Le Bellégo, J.F. Dubé, G. Pijaudier-Cabot, B. Gérard, Calibration of nonlocal damage model from size effect tests. European Journal of Mechanics A/Solids, 22 (2003) 33–46.
[2] S. Kumar, S.V. Barai, Concrete fracture models and applications, Springer-Verlag, Berlin Heidelberg, 2011.
[3] G.R. Irwin, Plastic zone near a crack and fracture toughness. Sagamore Research Conference Proceedings, Vol. 4, 1961.
[4] S. Xu, H.W. Reinhardt, Determination of double-K criterion for crack propagation in quasibrittle materials, Part II: Analytical evaluating and practical measuring methods for three-point bending notched beams. Int. J. Fract., 98 (1999) 151–77.
[5] ASTM E561–10, Standard Test Method for K-R Curve Determination. Annual book of standards, Volume 03.01. ASTM International West Conshohocken, PA, 2011.
[6] Z.P. Bažant, J. Planas, Fracture and size effect in concrete and other quasibrittle materials, CRC Press, Florida, 1998.
[7] Z.P. Bažant, P.A. Pfeiffer, Determination of fracture energy from size effect and brittleness number. ACI Materials Journal, 84 (1987) 463–80.
[8] K.R.W. Wallin, Critical assessment of the standard ASTM E 399. J. ASTM Int., 2, (2005).
[9] K.R.W. Wallin, Fracture toughness of engineering materials - estimation and application, EMAS Publishing, Warrington UK, 2011.
[10] B.L. Karihaloo, P. Nallathambi, Fracture toughness of plain concrete from three-point bend specimens. Materials and Structures/Matériaux et Constructions, 22, (1989). 85–93.
[11] T.M.E. Refai, S.E. Swartz, Fracture behavior of concrete beams in three-point bending considering the influence of size effects, Report No. 190, Engineering Experiment Station, Kansas State University; 1987.
[12] C.G. Go, S.E. Swartz, Energy methods for fracture-toughness determination in concrete. Exp. Mech., 26, (1986), 292–6.
[13] Z.P. Bažant, R. Gettu, M.T. Kazemi, Identification of nonlinear fracture properties from size effect tests and structural analysis based on geometry-dependent R-curves, Int. J. Rock Mech. Min. Sci. & Geomech. Abstr., 28, (1991) 43–51.
[14] Z. Wu, S. Yang, X. Hu, J. Zheng, An analytical model to predict the effective fracture toughness of concrete for three-point bending notched beams, Engng. Frac. Mech., 73, (2006),

2166–2191.
[15] S.T. Yang, X.Z. Hu, Z.M. Wu, Influence of local fracture energy distribution on maximum fracture load of three-point-bending notched concrete beams, Engng. Frac. Mech., 78, (2011), 3289–3299.